

Supporting Information

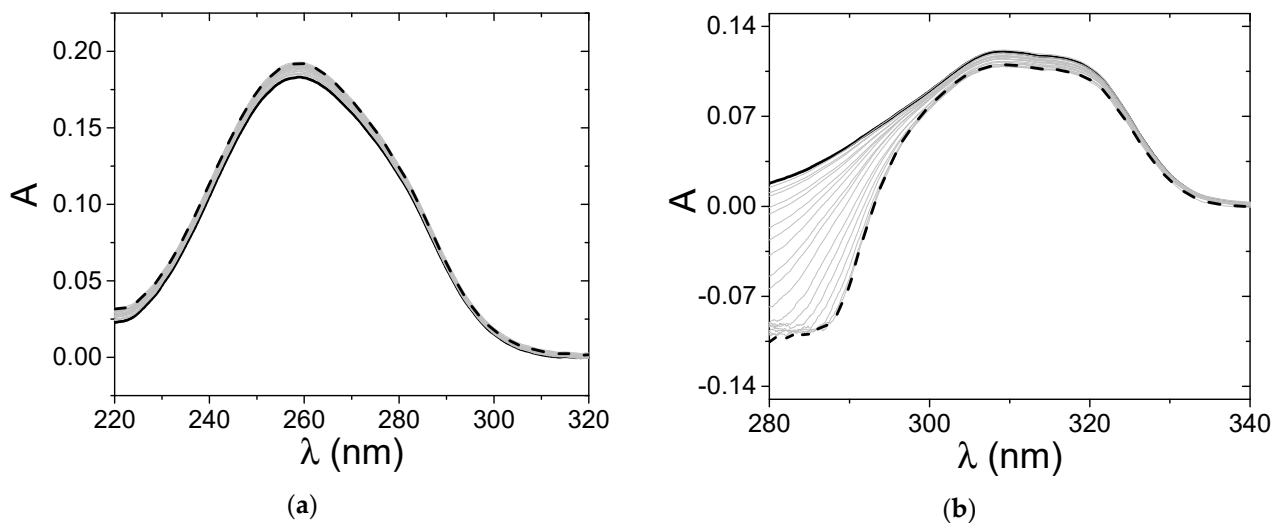


Figure S1. Spectrophotometric titrations of (a) PQ/DNA ($C_{PQ} = 9.30 \times 10^{-6}$ M, C_{DNA} from 0 (solid) to 6.49×10^{-4} M (dash)) and (b) DQ/DNA ($C_{DQ} = 6.87 \times 10^{-6}$ M, C_{DNA} from 0 (solid) to 7.71×10^{-6} M (dash)). NaCl 0.1 M, NaCac 2.5 mM, pH 7.0, 37.0°C.

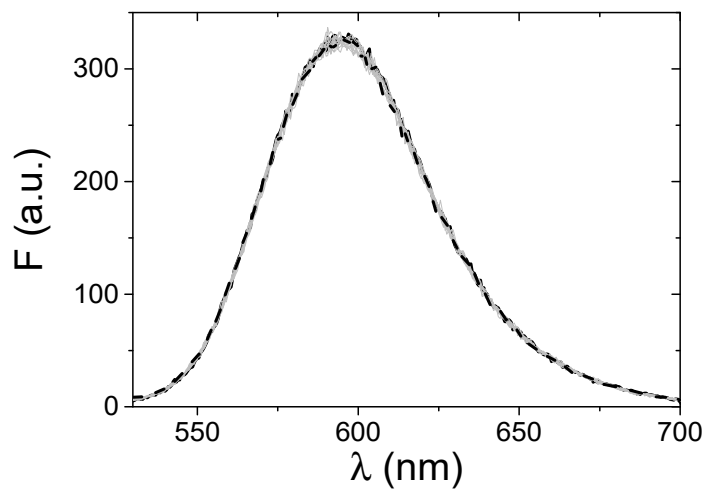


Figure S2. Fluorescence exchange titration of EtBr-saturated DNA with DQ at 25.0°C ($C_{EtBr} = 9.96 \times 10^{-5}$ M, $C_{DNA} = 2.43 \times 10^{-4}$ M, C_{DQ} from 0 (solid) to 8.03×10^{-4} M (dash), NaCl 0.1 M, NaCac 2.5 mM, pH 7.0, 25.0°C, $\lambda_{exc} = 510$ nm, $\lambda_{em} = 595$ nm).

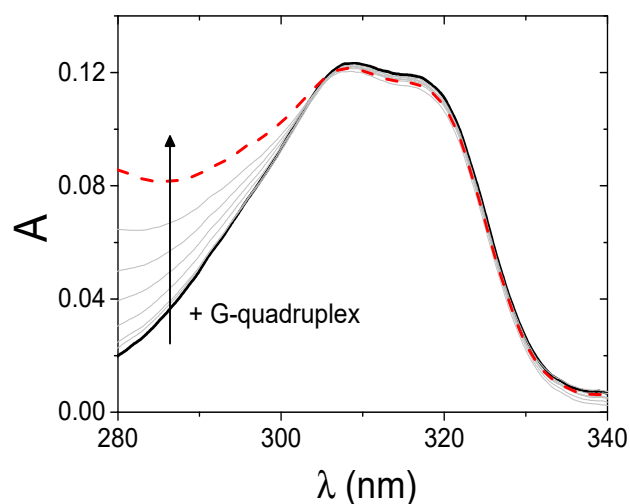


Figure S3. Spectrophotometric titration for the Tel23-DQ system; $C_{\text{Tel}} = 7.77 \times 10^{-9}$ (—) – 5.00×10^{-7} M (---); $C_{\text{DQ}} = 8.87 \times 10^{-6}$ M, KCl 0.1 M, KCac 2.5 mM, pH 7.0, 25.0 °C.

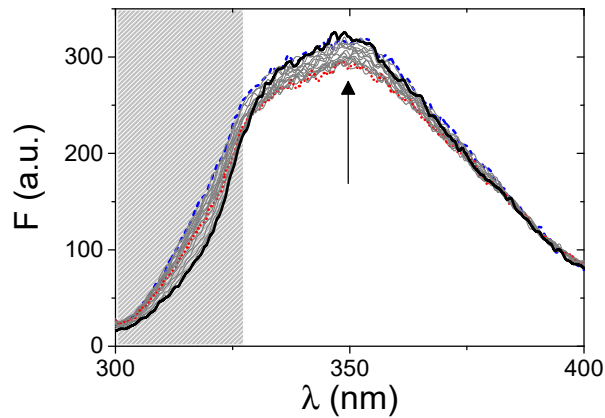


Figure S4. Spectrofluorimetric titration for the DQ/BSA system. The grey area highlights the distortions due to DQ absorbance effects. The arrow indicates the fluorescence emission profile likely due to free DQ contribution, which becomes evident for $C_{\text{DQ}} > 1.86 \times 10^{-6}$ M; accordingly, the binding isotherm in Figure 7 is cut at $C_{\text{DQ}} < 1.86 \times 10^{-6}$ M; $C_{\text{BSA}} = 1.50 \times 10^{-6}$ M, C_{DQ} from 0 (dashed blue line) to 1.86×10^{-6} M (dotted red line) and 1.07×10^{-5} M (straight black line), NaCl 0.1 M, NaCac 2.5 mM, pH 7.0, 37.0°C, $\lambda_{\text{exc}} = 295$ nm.

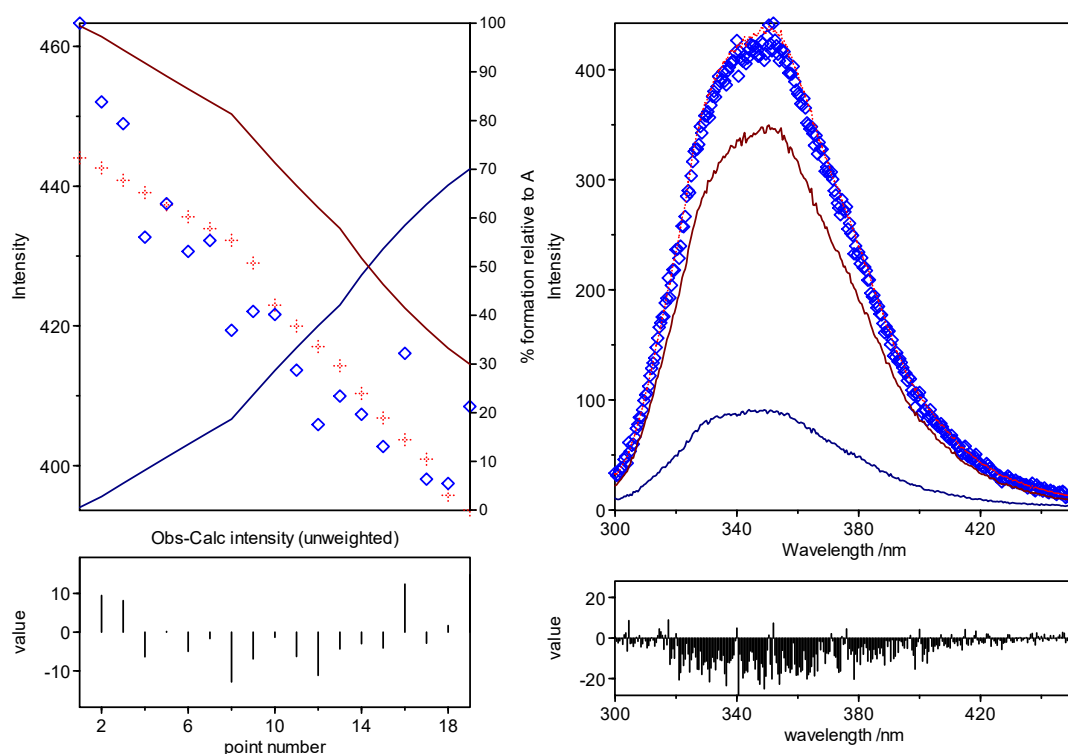


Figure S5. HypSpec2014 analysis of the fluorescence changes observed upon addition of DQ to BSA; $C_{\text{BSA}} = 1.50 \times 10^{-6}$ M, C_{DQ} from 0 to 1.77×10^{-6} M, NaCl 0.1 M, NaCac 2.5 mM, pH 7.0, 37.0°C, $\lambda_{\text{exc}} = 295$ nm. Left: titration curve at 345 nm (open diamond = experimental, cross = calculated) and species distribution (dark red = free BSA, red = PQ/BSA adduct). Right: fluorescence spectrum ((open diamond = experimental, dashed red line = calculated) and relevant deconvolution (dark red = free BSA, red = PQ/BSA adduct). The bottom panels are the residuals.

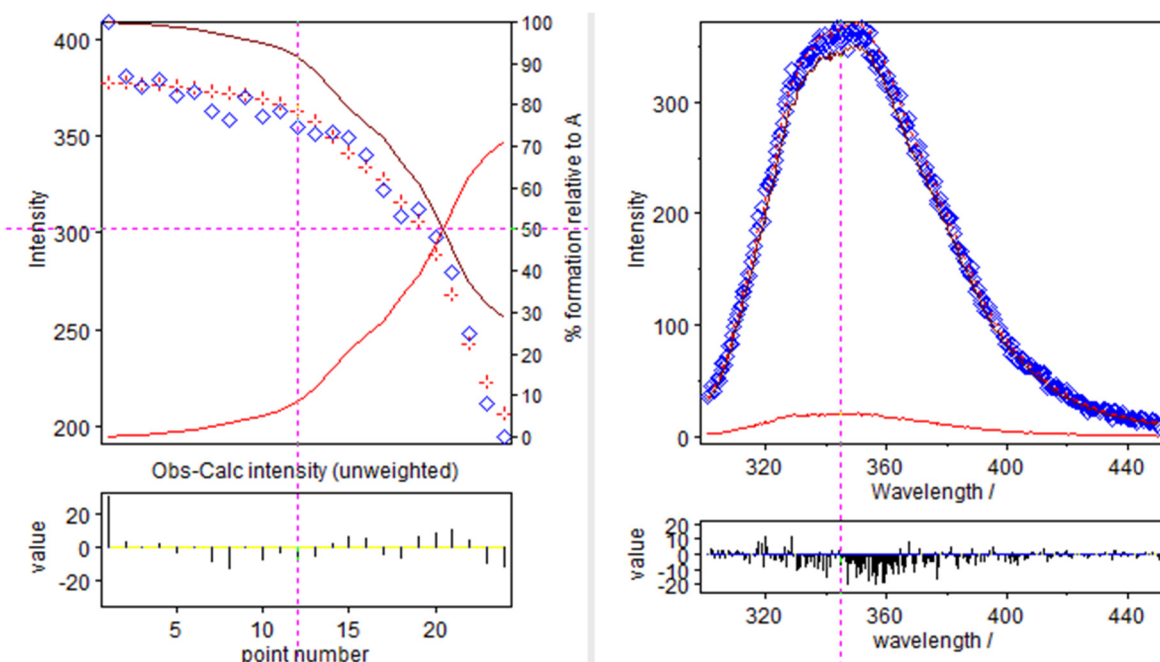


Figure S6. HypSpec2014 analysis of the fluorescence changes observed upon addition of PQ to BSA; $C_{\text{BSA}} = 1.54 \times 10^{-6}$ M, C_{PQ} from 0 to 5.12×10^{-5} M, NaCl 0.1 M, NaCac 2.5 mM, pH 7.0, 37.0°C, $\lambda_{\text{exc}} = 295$ nm. Left: titration curve at 345 nm (open diamond = experimental, cross = calculated) and species distribution (dark red = free BSA, red = PQ/BSA adduct). Right: fluorescence spectrum ((open diamond = experimental, dashed red line = calculated) and relevant deconvolution (dark red = free BSA, red = PQ/BSA adduct). The bottom panels are the residuals.

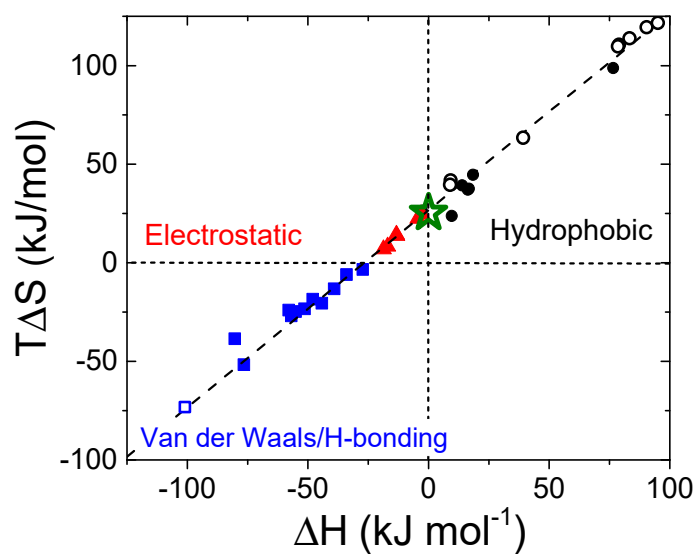


Figure S7. Plot of ΔH vs. $T\Delta S$ for different ligands binding to BSA according to <https://doi.org/10.1016/j.jinorgbio.2020.111305>. Different points relate to the different driving forces for binding: (●) = hydrophobic forces, (■) = van der Waals/H-bonding, (▲) = electrostatic. Full point refer to organic molecules, open points refer to metal complexes. The star refers to what was found in this work for the PQ/BSA system.

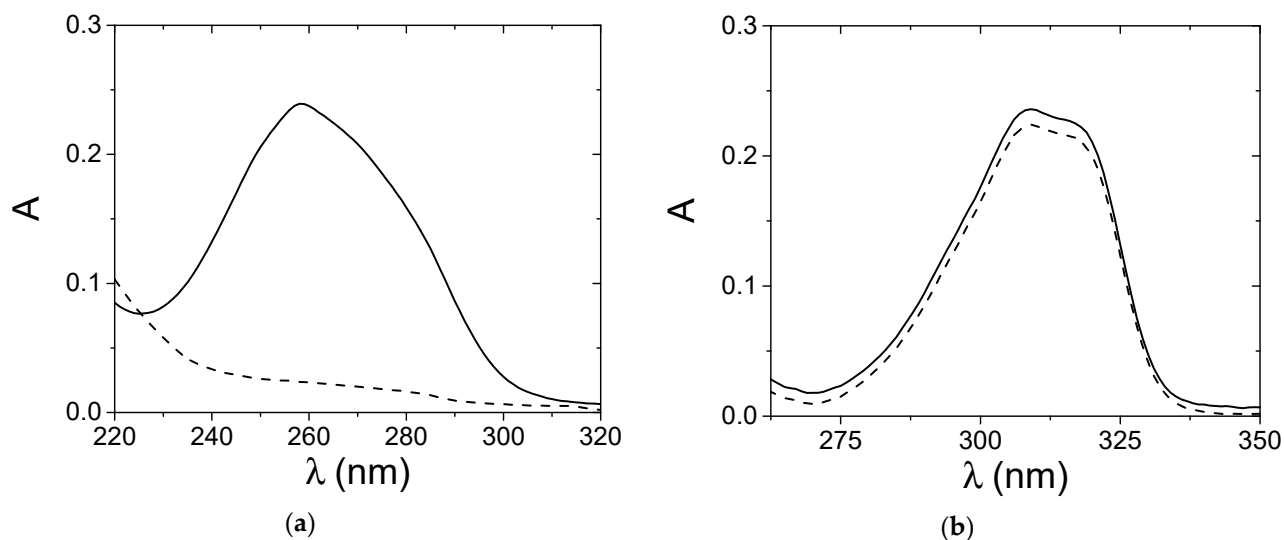


Figure S8. Absorbance spectra of (a) PQ in SDS 0.01 M before (solid) and after (dash) ultrafiltration and (b) DQ in DTAC 0.01 M before (solid) and after (dash) ultrafiltration; NaCl 0.1 M, NaCac 2.5 mM, pH 7.0.